

SOWAT: High-resolution imaging with only partial AO correction

Felix Bosco¹†, Jörg-Uwe Pott¹ and Rainer Schödel²

¹Max-Planck-Institut für Astronomie (MPIA), Königstuhl 17,
D-69117 Heidelberg, Germany
email: bosco@mpia.de

²Instituto de Astrofísica de Andalucía (IAA-CSIC), Glorieta de la Astronomía S/N,
E-18008 Granada, Spain

Abstract. Observations of dense stellar systems such as globular clusters (GCs) are limited in resolution by the optical aberrations induced by atmospheric turbulence (atmospheric seeing). At the example of holographic speckle imaging, we now study, to which degree image reconstruction algorithms are able to remove residual aberrations from a partial adaptive optics (AO) correction, such as delivered from ground-layer AO (GLAO) systems. Simultaneously, we study, how such algorithms benefit from being applied to pre-corrected instead of natural point-spread functions (PSFs). We find that using partial AO corrections already lowers the demands on the holography reference star by ~ 3 mag, what makes more fields accessible for this technique, and also that the discrete integration times may be chosen about $2\text{--}3\times$ longer, since the effective wavefront evolution is slowed down by removing the perturbation power.

Keywords. instrumentation: adaptive optics – instrumentation: high angular resolution – techniques: high angular resolution – techniques: image processing – techniques: photometric

1. Introduction

There are two common solutions for removing optical aberrations from astronomical observations, due to atmospheric turbulence. On telescopes with primary mirror diameters $\lesssim 2.5$ m, speckle imaging techniques such as lucky imaging provide diffraction limited observations, when reconstructing the short-exposure (typically $\lesssim 100$ ms) images with appropriate algorithms. For larger telescopes, such as modern 8m-class or future extremely large telescopes (ELTs), however, adaptive optics (AO) systems are indispensable tools, actively controlling the wavefront aberrations. Nowadays, most of the AO systems in use are either single-conjugate AO (SCAO) systems, typically providing PSF inhomogeneities even at small distances from the reference star, or partial AO systems, providing fairly homogeneous PSFs across the field of view (FoV) at the cost of the larger residual PSF width. Examples for such systems are, for instance, ground-layer conjugated AO (GLAO) systems using laser guide stars (LGSs), which are not able to correct for the aberrations induced by the higher layers of the atmosphere (e.g. LBT/ARGOS, [Rabien et al. 2010](#)), or mode-restricted single-conjugate AO systems, which correct only for a limited number of (low) Zernike modes and thus work with fainter reference stars (e.g. LBT/ESM, [Rothberg et al. 2018](#)).

As part of the SOWAT project (Speckle Observations With Alleviated Turbulence; [Bosco, Pott & Schödel 2019](#), hereafter BPS19), we study the benefits of combining (advanced) lucky imaging algorithms with partial AO corrections, available at most of

† Fellow of the International Max Planck Research School on Astronomy and Cosmic Physics at the University of Heidelberg

Table 1. AO system simulations.

Label	Description	PSF width (arcsec)	Template
noAO	natural seeing	1.00	Natural seeing at 500 nm
ESM	mode-restricted SCAO	0.75	LBT/ESM (Rothberg <i>et al.</i> 2018)
GLAO	ground-layer AO	0.45	LBT/ARGOS (Rabien <i>et al.</i> 2010)
SCAO	single-conjugate AO	0.05	–

the 8m-class telescopes. For a more detailed description of the project, we refer to that publication and provide a brief overview of the key insights in this article.

2. Simulations and residual wavefront evolution

We simulate short-exposure PSFs of 8m-class telescopes with the end-to-end simulation tool YAO (Rigaut & Van Dam 2013). We consider different designs of AO systems as summarized in Table 1, where the single-conjugate AO (SCAO) setup was used only for reference. The particular parameters of each simulation are summarized in Table 1 and 2 of BPS19.

Analyzing the residual wavefronts delivered from these observations, we study the difference in the wavefront decorrelation behavior. In Fig. 3 of BPS19, the differences between natural and AO-controlled wavefront evolution are easily recognizable. Measuring the mean standard deviation of the difference of two randomly selected snapshots of the residual wavefront and plotting this quantity as a function of time span between the two frames shows functions of bounded growth. The time scale and limit of these bounded growth processes are defined by the respective time scale and power of the residual modes of the atmospheric perturbation.

3. Synthetic observations and expected increase in S/N

With the simulated PSFs and the PYTHON package VEGAPy (see description in Sect. 2.2 of BPS19), we generate synthetic observations of an artificial star cluster, including realistic photon and readout noise. The simulated discrete integration times (DITs) range from 200 ms up to 2.5 s.

For the holographic reconstruction, it is important to obtain a high signal-to-noise ratio (S/N) in the absolute squared of the Fourier transform, i.e. the power spectrum, of the PSF estimate, to avoid division by small values. We estimate the S/N of these power spectra for holographic reference stars of *H*-band magnitudes 12, 14 and 16 as a function of spatial wavelength. In Fig. 1, we compare the functions obtained from different AO system designs to that obtained for natural seeing and find that the mode-restricted AO (ESM, top panel) increases the S/N of the long spatial wavelengths, which is expected as these are mostly affected by the long Zernike modes filtered out by the ESM. Since the GLAO system (bottom panel) is not restricted to a particular mode, it increases the S/N also towards shorter spatial wavelengths. However, the uncorrected higher atmospheric layers still contribute fluctuations at the long spatial scales.

4. Impact on image quality

We compare the result of the holographic image reconstruction algorithm (Schödel & Girard 2012; Schödel *et al.* 2013) on the synthetic images and compare the results to a conventional simple shift-and-add (SSA, Bates & Cady 1980) reconstruction, in Fig. 2. The image quality is measured by the encircled energy as a function of aperture radius around the star.

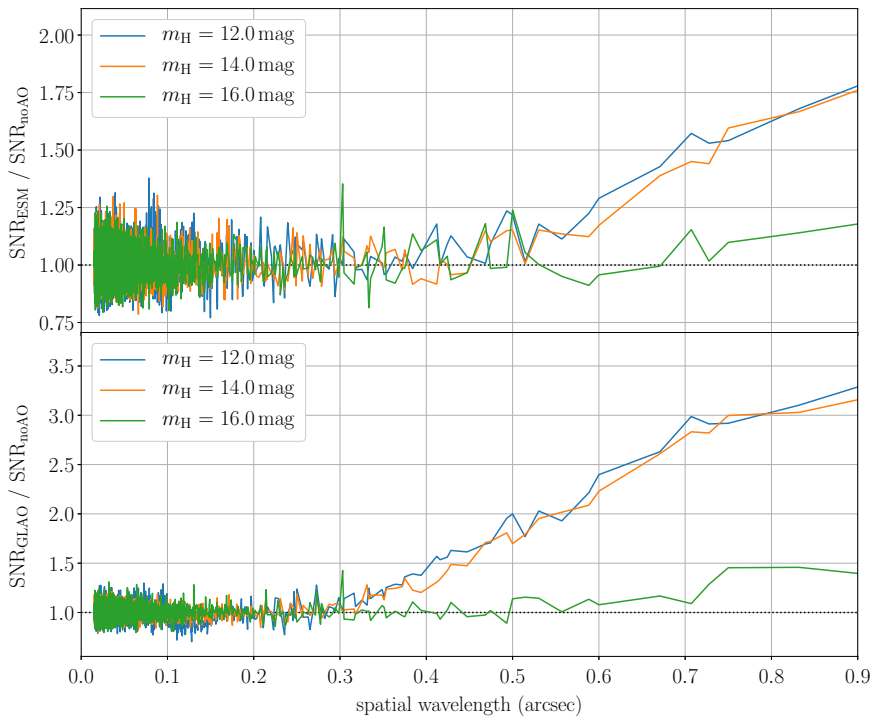


Figure 1. Gain in the SNR of the power spectra for a ESM (*top*) and GLAO (*bottom*) wavefront control versus no control (noAO), as a function of spatial wavelength in the aperture and for three stellar magnitudes. The dotted black line indicates a ratio of order unity. Adapted from BPS19.

The advantage of the holographic image reconstruction over the conventional algorithm becomes particularly prominent as the central peak of the Airy function (expressing diffraction limited observations) causes a steep rise within the central three pixels. Both reconstructions benefit from using the partial AO correction, which is expected in the SSA reconstruction, since every single short-exposure PSF itself is expected to be more focused and thus also the alignment of these PSFs is more focused towards the central position of the star. In the less linear holographic approach, this is, however, predominantly due to the fact that the S/N of the PSF estimate power spectra is increased significantly as described in Sect. 2. But also the integration time increases the S/N of the power spectra (cf. Fig. 5 of BPS19) and therefore, the holographic reconstruction also benefits from longer integration times. We note that, in practice, this may come with the penalty of not resolving close binaries if the aperture around the holography reference star contains the binary companion. This issue may be solved, however, if a median superposition of multiple reference stars are chosen (Schödel *et al.* 2013).

5. Summary

We summarize that short-exposure image reconstruction algorithms in general benefit from being applied to data obtained with the aid of (partial) AO corrections. Using advanced image reconstruction algorithms such as speckle holography additionally overcomes the penalty of PSF smearing and thus enables in combination with partial AO corrections longer integration times. Our simulations of such observing modes suggest that *long-exposure speckle imaging* with DITs $\gtrsim 1$ sec are possible.

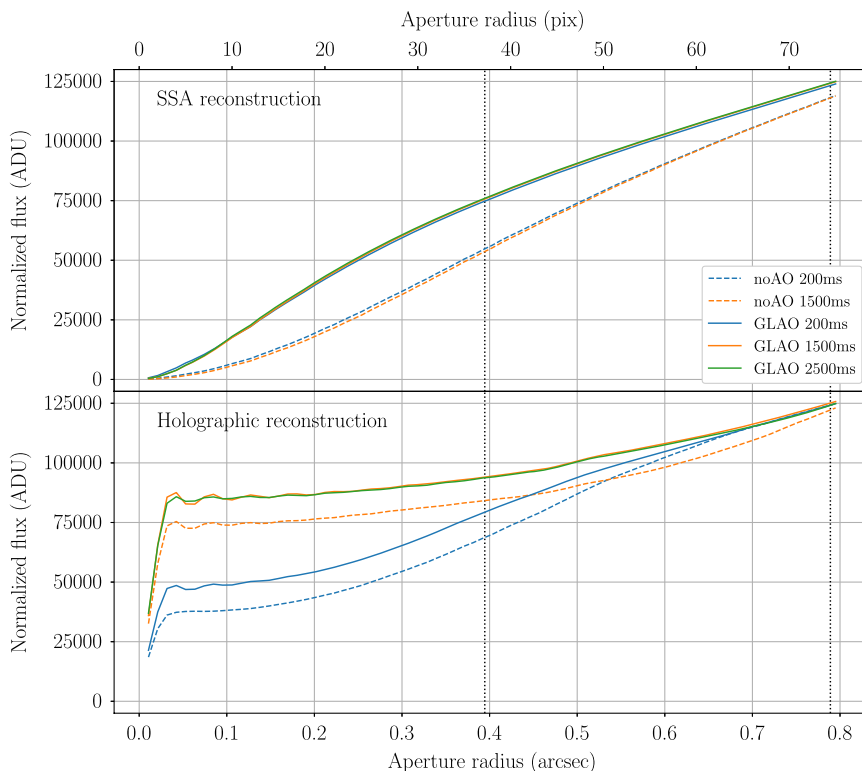


Figure 2. Encircled energy in the reconstruction of the synthetic data sets around a $H = 12.4$ mag star, for the case of simple-shift-and-add reconstruction (*top*) and holographic reconstruction (*bottom*). The flux is normalized to the total integration time of 160 s. The dotted vertical lines indicate one and two times the expected HWHM in H -band, corresponding to $R_{\text{aperture}} = 0.4$ and 0.8 arcsec, respectively. Adapted from BPS19.

References

- Bates, R. H. T. & Cady, F. M. 1980, *Optics Communications*, 32, 365, 10.1016/0030-4018(80)90261-8
- Bosco, F., Pott, J.-U., & Schödel, R. 2019, *PASP*, 131, 044502
- Noll, R. J. 1976, *Journal of the Optical Society of America (1917–1983)*, 66, 207
- Rabien, S., Ageorges, N., Barl, L., *et al.* 2010, *Proceedings of SPIE*, Vol. 7736, Adaptive Optics Systems II, 77360E–77360E–12
- Rigaut, F. & Van Dam, M. 2013, *Proceedings of the Third AO4ELT Conference*, ed. S. Esposito & L. Fini, 18
- Rothberg, B., Kuhn, O., Power, J., *et al.* 2018, in *Society of Photo-Optical Instrumentation Engineers (SPIE) Conference Series*, Vol. 10702, Ground-based and Airborne Instrumentation for Astronomy VII, 1070205
- Schödel, R. & Girard, J. H. 2012, *Messenger*, 150, 26
- Schödel, R., Yelda, S., Ghez, A., *et al.* 2013, *MNRAS*, 429, 1367